

Original Article

Ultrastructural changes in fetal rat testes after mono(2-ethylhexyl)phthalate exposure *in vitro*

Tong-Dian Zhang^{1*}, Lian-Dong Zhang^{1*}, Li-Li Xu², Yu-Bo Ma¹, He-Cheng Li¹, Zi-Ming Wang¹

¹Department of Urology, The Second Affiliated Hospital, Xi'an Jiaotong University, Xi'an 710004, Shaanxi, China;

²Department of Gynecological, Liaocheng Tumor Hospital, Liaocheng 252000, Shandong, China. *Equal contributors.

Received February 16, 2020; Accepted April 24, 2020; Epub June 15, 2020; Published June 30, 2020

Abstract: Exposure to Mono(2-ethylhexyl)phthalate (MEHP) is known to impair the normal development of fetal testis, resulting in reproductive tract disorders such as Sertoli-cell-only syndrome, hypospadias, cryptorchidism, and impaired spermatogenesis. The embryonic period is particularly important for the development of the male reproductive system. However, the exact changes in fetal testis after MEHP exposure are not well characterized. In this research, testes of 16.5 days post-conception (dpc) rat fetuses were isolated and cultured in the fetal testis assay system. At 3, 6, and 9 h after exposure to MEHP at different concentrations (0, 10 μ M and 100 μ M, respectively), apoptotic gene expressions were assessed and ultrastructural studies were conducted. Exposure to MEHP induced upregulation of Bax and Caspase-3 expression and downregulation of Bcl-2 expression. In addition, MEHP caused time- and dose-dependent mitochondrial degeneration in Sertoli cells and gonocytes characterized by swelling and loss of cristae. Apoptotic and necrotic cells were also detected after MEHP treatment. The apoptotic Sertoli cells exhibited marginated and condensed chromatin. Multinucleated gonocytes (MNGs) and increased electron density of gonocytes were identified after high-dose MEHP treatment. Moreover, broken basement membrane and intratubular Leydig cells (ITLCs) were found in the seminiferous tubules. To conclude, MEHP treatment tended to induce apoptosis or necrosis of gonocytes and Sertoli cells; high-dose MEHP tended to induce the occurrence of MNGs and ITLCs.

Keywords: Apoptosis, mono(2-ethylhexyl)phthalate, rat, testis, ultrastructure

Introduction

During the past 30 years, there are increasing reports about poor sperm quality, which are believed to result from exposure to endocrine-disrupting chemicals (EDCs) [1, 2]. Phthalate esters, a common class of EDCs, have raised wide concerns. In particular, di-(2-ethylhexyl) phthalate (DEHP) is the most frequently used plasticizer in the plastics industry; thus, it is found in many daily commodities, such as toys, water bottles, tableware, and medical equipment. Upon ingestion, DEHP is rapidly metabolized by esterases in the gut and other tissues, leading to the production of corresponding active monoesters, such as MEHP, a testicular toxicant [3].

The embryonic period is a particularly important period for the development of the male

reproductive system [4]. The development and differentiation of germ cells is a closely regulated process in which endocrine and paracrine signals play an important role [5, 6]. The gonocytes are precursors of type A spermatogonia and spermatogonial stem cells (SSCs) which determine the spermatogenic function of the adult [7, 8]. The fetal period is highly sensitive to EDCs, which can traverse the placental barrier and enter the genital ridge [9]. In the past 30 years, the fetal testis assay (FeTA) system has been developed, which allows the maintenance of gametogenesis and steroidogenesis of rat fetal testis tissues [10, 11]. MEHP exposure has been shown to induce a series of male reproductive disorders, including a reduction in testosterone, decreased proliferation and increased apoptosis of gonocytes, as well as the occurrence of vacuolated Sertoli cells [4, 12, 13].

Ultrastructural changes in rat testes after MEHP exposure

Despite increasing evidence related to the reproductive toxicity of phthalates, relatively few studies have evaluated the ultrastructural changes of fetal testes after exposure to EDCs. Light microscopy does not provide adequate and precise histological characterization, while electron microscopy facilitates elucidation of subtle intracellular changes that are more directly related to the physiological processes. In this study, we conducted ultrastructural studies to evaluate the toxicity of MEHP on fetal testes.

Materials and methods

Animals and sample collection

The experiments and protocol were approved by the Committee on Animal Research and Ethics of the Xi'an Jiaotong University (Xi'an, China) and were carried out in accordance with the Guidelines for Animal Experimentation of Xi'an Jiaotong University and the Guide for the Care and Use of Laboratory Animals published by the US National Institutes of Health (NIH Publication NO. 85-23, revised 2011). Two male and 12 female adult specific pathogen-free Sprague-Dawley rats were obtained from the Experimental Animal Center of Xi'an Jiaotong University and housed under controlled photoperiod conditions (lights on 08:00 h-20:00 hr) with ad libitum access to tap water and a soy-free breeding diet. Female rats were subjected to vaginal smear examination to estimate the estrous cycle. Female rats which were in proestrus and estrus were caged overnight with male rats in a ratio of 2:1. The vaginal smear was performed again the next day. The presence of sperm in the smear was indicative of 0.5 dpc. On 16.5 dpc, pregnant female Sprague-Dawley rats were anesthetized by intraperitoneal injection of 2% sodium pentobarbital (Sigma-Aldrich Inc., St. Louis, MO, U.S.A.; 0.2 ml/100 g body weight). The fetal testes were isolated aseptically from the 16.5 dpc fetuses under an anatomical microscope and then immediately explanted in vitro.

Organ culture and exposure

Testes were cultured on Millicell-CM Biopore membranes (Millipore Corp., Bedford, MA, U.S.A.) [14]. The culture solution was phenol red-free F12/Dulbecco's Modified Eagle's Medium (DMEM/F12) (Gibco, Grand Island, NY,

U.S.A.) supplemented with 10% Knockout™ Serum Replacement (KSR) (Gibco, Grand Island, NY, U.S.A.), penicillin (100 IU/ml) and streptomycin (100 IU/ml) (TransGen Biotech, Beijing, China). MEHP (Accustandard Inc., New Haven, CT, U.S.A.) was dissolved in 99.5% pure dimethylsulfoxide (DMSO) (Sigma-Aldrich Inc., St. Louis, MO, U.S.A.) to prepare stock solutions of 100 mM. Testes were exposed to vehicle (control), MEHP (10, 100 μ M, respectively), and the final concentration of DMSO in each group was 0.1%. The cultured testes were incubated at 37°C in a humidified atmosphere of 95% air and 5% carbon dioxide. The harvesting was carried out at 3, 6, and 9 hr after culture; nine groups were formed in this study (CTRL3, 10 μ M3, 100 μ M3; CTRL6, 10 μ M6, 100 μ M6; CTRL9, 10 μ M9, 100 μ M9). Twelve testes were used in each group, and 6 testes in each group were used for real time quantitative polymerase chain reaction (RT-qPCR) and transmission electron microscopy, each.

In a pilot study, 10 μ M of MEHP was added to the culture system, and only 0.3% of MEHP was present in the cultured testis; this corresponds to a concentration of approximately 2500 μ g/l, which is relevant to the environmental exposure in humans [12, 15]. The no observable adverse effect level (NOAEL) of MEHP for human germ cells ranges between 1 μ M and 10 μ M [13]. The maximal concentration of MEHP in neonatal cord blood samples is 10 μ M (mean value: 2 μ M) [16]. Moreover, the mean concentration of MEHP in fetal cord blood samples is approximately 36 μ M [17]. In the clinical setting, such as exposure to DEHP from a blood transfusion, the concentration of MEHP in fetal cord blood can be as high as one to two orders of magnitude over the general exposure level [18]. Therefore, the relevant doses of 10 μ M and 100 μ M were chosen in this study.

RNA extraction and RT-qPCR

Total RNA was extracted from fetal testis using a total RNA extraction kit (Fastagen Biotech Co., Ltd., Shanghai, China) and then reverse transcribed using RevertAid™ First Strand cDNA synthesis kit (Thermo Fisher Scientific, Inc., Waltham, MA, U.S.A.). RT-qPCR was performed using the Bio-Rad Real-Time PCR system (IQ5; Bio-Rad). GAPDH was used as an endogenous control. Relative gene expression was analyzed using a $2^{-\Delta\Delta Cq}$ algorithm. Primers

Ultrastructural changes in rat testes after MEHP exposure

Table 1. Gene-specific primers used in the study

Gene name	Accession no.	Specific primer (5' to 3')
Caspase-3	NM_012922.2	Forward: TGGAACGAACGGACCTGTG Reverse: CGGGTGC GG TAGAGTAAGC
Bax	NM_017059.2	Forward: CAGGATGCGTCCACCAAGAA Reverse: CGTGTCCACGTCAGCAATCA
Bcl-2	NM_016993.1	Forward: GGGATGCCTTTGTGGA ACTATATG Reverse: TGAGCAGCGTCTTCAGAGACA
GAPDH	NM_017008.4	Forward: TGGGTGTGAACCACGAGAA Reverse: GGCATGGACTGTGGTCATGA

Bcl-2: B-cell lymphoma-2, Bax: Bcl-2-associated x protein, GAPDH: glyceraldehyde-3-phosphate dehydrogenase.

satisfied the following criteria: melting temperature (T_m), approximately 60-64°C; GC content, approximately 35-65%. All primer sequences for gene targets are listed in **Table 1**.

Transmission electron microscope

The harvested-testes were promptly washed with 0.1 M phosphate buffer saline (PBS), immersed in 2.5% glutaraldehyde plus 4% paraformaldehyde in phosphate buffer for 2 h at 4°C. Then, the testes were washed with 0.1 M phosphate buffer for 30 min, postfixed in 1% osmium tetroxide in phosphate buffer for 2 hr at 4°C, washed for 20 minutes with PBS again, dehydrated in a graded series of ethanol (30, 50, 70, 80, 90, 95, and 100% ethanol), immersed overnight in a mixture of propylene oxide plus epon 812 at 37°C, and embedded in polymerization. Ultrathin sections were stained with uranyl acetate and lead hydroxide and examined with a HITACHI H-7650 transmission electron microscope at 80 kV.

Statistical analysis

Data are presented as mean \pm standard error of the mean (SEM) and analyzed using GraphPad Prism 5 (GraphPad, USA). Statistical analysis was conducted using one-way analysis of variance, followed by Tukey's test. P values <0.05 were indicative of statistical significance.

Results

In vitro exposure to MEHP altered the expression of apoptotic genes

The expressions of apoptotic genes (Caspase-3, Bax, and Bcl-2) in each group are presented in

Figure 1. Exposure to 10 μ M MEHP for 3, 6, and 9 hr and 100 μ M MEHP for 6 and 9 hr caused a significant increase in Caspase-3 expression compared with corresponding control ($P<0.05$). Moreover, exposure to 10 μ M MEHP for 9 hr caused a significant increase in Caspase-3 expression compared with 10 μ M MEHP exposure for 3 hr ($P<0.05$). Exposure to 100 μ M MEHP for 9 hr caused a significant increase in Caspase-3 expression compared with 100 μ M MEHP exposure for 3 and 6 hr and

10 μ M MEHP exposure for 9 hr ($P<0.05$). Exposure to 100 μ M MEHP for 6 and 9 hr caused a significant increase in Bax expression compared with corresponding control ($P<0.05$). Exposure to 100 μ M MEHP for 9 hr caused a significant increase in Bax expression compared with 100 μ M MEHP exposure for 3 hr, and that of 10 μ M MEHP exposure for 9 hr ($P<0.05$). Exposure to 100 μ M MEHP for 3, 6, and 9 hr and that of 10 μ M MEHP for 9 hr caused a significant decrease in Bcl-2 expression compared with the corresponding control ($P<0.05$). Exposure to 10 μ M MEHP for 9 hr caused a significant decrease in Bcl-2 expression compared with 10 μ M MEHP exposure for 3 hr ($P<0.05$).

Effects of MEHP exposure on Sertoli cell ultrastructure

Figure 2A and **2B** show the ultrastructure of Sertoli cells in the control group; no morphological defects were seen after culture. Sertoli cells showed normal morphological characteristics, including regularly shaped nuclei and a number of mitochondria and rough endoplasmic reticula. Ten μ M MEHP treatment for 3 hr caused no degenerative changes in Sertoli cells (data not shown). After 10 μ M MEHP treatment for 6 hr and 100 μ M MEHP for 3 hr, swollen mitochondria were observed in Sertoli cells (**Figure 2C, 2D**). After 10 μ M MEHP treatment for 9 hr, apoptotic Sertoli cells were identified in seminiferous tubules (**Figure 2E**). Apoptotic Sertoli cells were characterized by cytoplasm shrinkage with still functioning cell organelles and no membrane rupture. The nuclei of apoptotic Sertoli cells were densely packed with marginated and condensed chromatin (**Figure 2E**). One hundred μ M MEHP treatment for 6 and 9 hr caused more advanced alterations,

Ultrastructural changes in rat testes after MEHP exposure

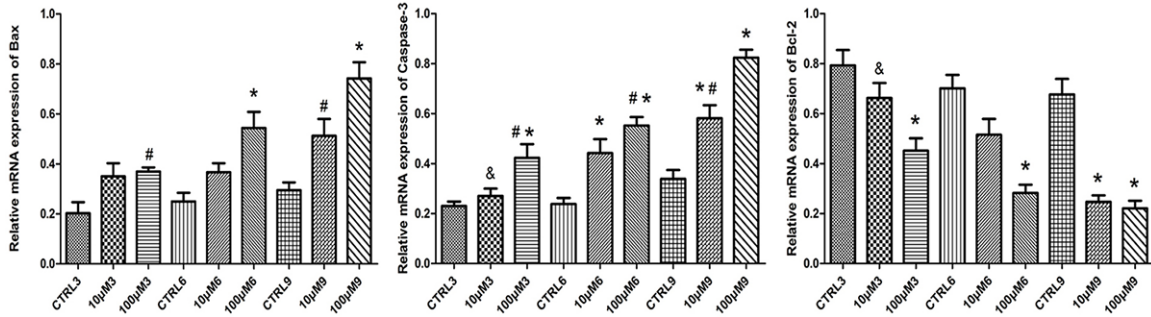


Figure 1. MEHP-induced changes in the mRNA levels of apoptosis-related genes. * $P < 0.05$ vs. corresponding CTRL; # $P < 0.05$ vs. 100 μM ; & $P < 0.05$ vs. 10 μM . Data presented as mean \pm SE.

and necrotic Sertoli cells were identified (**Figure 2F**). Necrotic Sertoli cells were characterized by ruptured mitochondria, plasma membrane lysis, as well as spilt cell contents.

Effects of MEHP exposure on gonocytes ultra-structure

In the control group, normal gonocytes were observed in the seminiferous tubules with extensive mitochondria, rough endoplasmic reticulum, and ribosomes (**Figure 3A, 3B**). Ten μM MEHP treatment for 3 and 6 hr did not induce any degenerative changes in the gonocytes (data not shown). After 10 μM MEHP treatment for 9 hr, swollen mitochondria were observed in gonocytes (**Figure 3C**). After 100 μM MEHP treatment for 3 hr, apoptotic gonocytes were identified in seminiferous tubules (**Figure 3D**). Apoptotic gonocytes were characterized by cytoplasmic shrinkage and condensed chromatin (**Figure 3D**). After 100 μM MEHP treatment for 6 and 9 hr, large multinucleated gonocytes (MNGs) were observed (**Figure 3E**), while some of the gonocytes showed increased electron density (**Figure 3F**).

Apoptotic cells and apoptotic body

After 10 μM MEHP treatment for 9 hr and 100 μM MEHP treatment for 6 and 9 hr, some apoptotic cells were found to have been swallowed by the adjoining Sertoli cells (**Figure 4A, 4B**). We also found a Sertoli cell in the process of swallowing an apoptotic cell (**Figure 4C**). Typical apoptotic bodies that originated from apoptotic cells were seen in the seminiferous tubules (**Figure 4D**).

Effects of MEHP exposure on Leydig cell and basement membrane

In the control group, normal fetal Leydig cells were observed, and the basement membrane was complete (**Figure 5A**). After 100 μM MEHP treatment for 9 hr, all of the degenerative changes stated above were observed. The number of necrotic and apoptotic cells tended to gradually increase in a time- and dose-dependent manner. Furthermore, the basement membrane of some seminiferous tubules was broken, and some Leydig cells referred to as intratubular Leydig cells (ITLCs) were aberrantly located inside the seminiferous tubules (**Figure 5B, 5C**).

Discussion

Apoptosis is a highly regulated process of cell death, which plays an important role in balancing cell proliferation and differentiation [19]. The Bcl-2 family of proteins includes several crucial apoptosis regulatory factors [20]. While Bcl-2 is an antiapoptotic protein, Bax is a proapoptotic protein. Caspases are a classic family of cysteinyl aspartate proteinases which are mainly involved in apoptosis. Among the downstream caspases, Caspase-3 plays a critical role in mediating apoptosis. In this study, MEHP increased the mRNA expression levels of Caspase-3 and Bax, and decreased the level of Bcl-2 in a time- and dose-dependent manner; these findings indicate that MEHP may induce apoptosis in testicular tissue.

In the control group, fetal testes showed normal ultrastructure after culture. Sertoli cells were mostly situated at the basal lamina,

Ultrastructural changes in rat testes after MEHP exposure

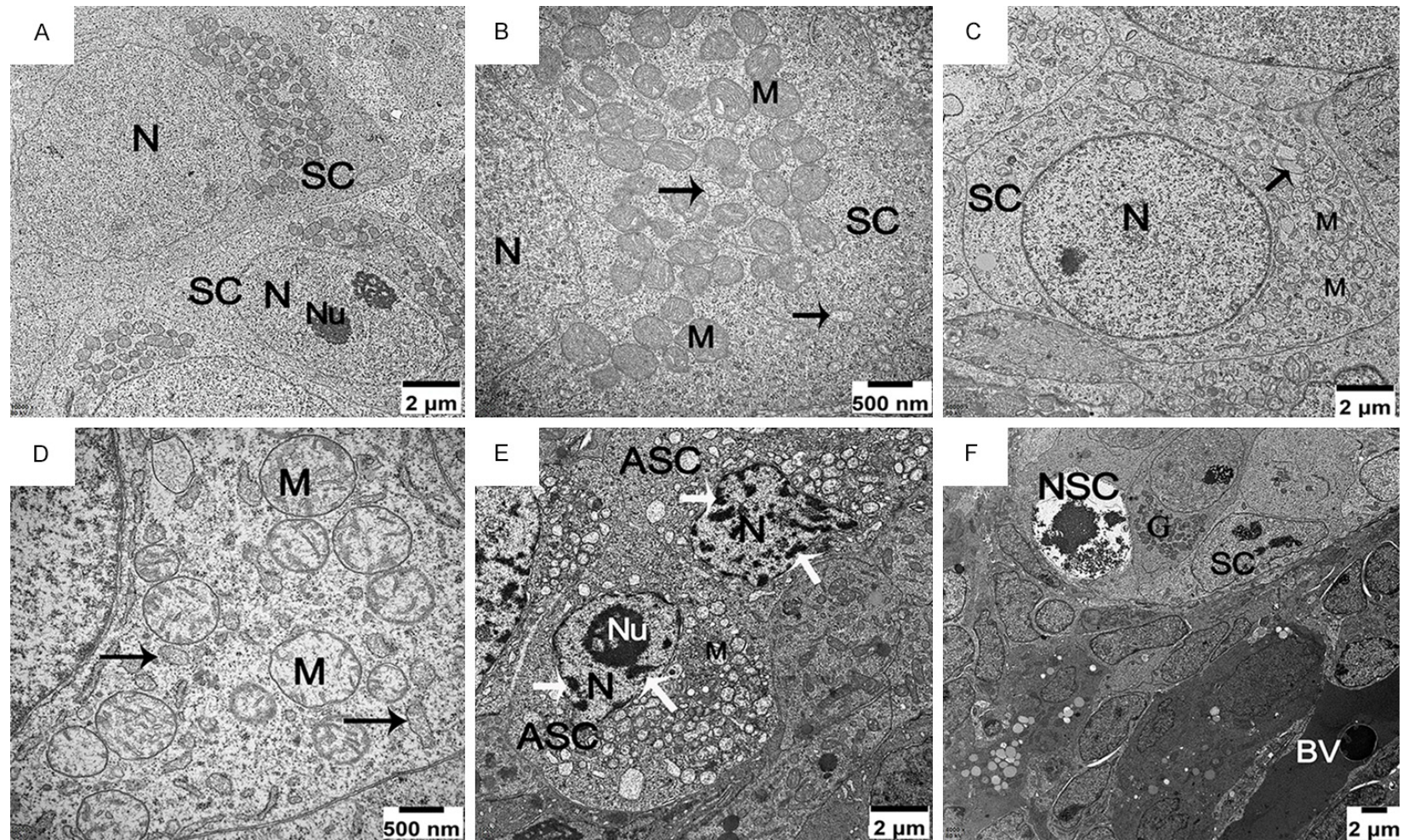


Figure 2. Degenerative changes in Sertoli cells (SC) after MEHP treatment. A, B. Normal ultrastructure of Sertoli cells was seen in the control group with normal ultrastructure of mitochondria (M) and endoplasmic reticulum (black arrow). C, D. Swollen mitochondria with loss of cristae were seen after MEHP treatment. E, F. Apoptotic Sertoli cells (ASC) and necrotic Sertoli cells (NSC) were also identified after MEHP treatment. Chromatin condensed in margin (white arrow) was seen in the nuclei (N) of ASCs. Nu: nucleolus, G: gonocyte, BV: blood vessel.

Ultrastructural changes in rat testes after MEHP exposure

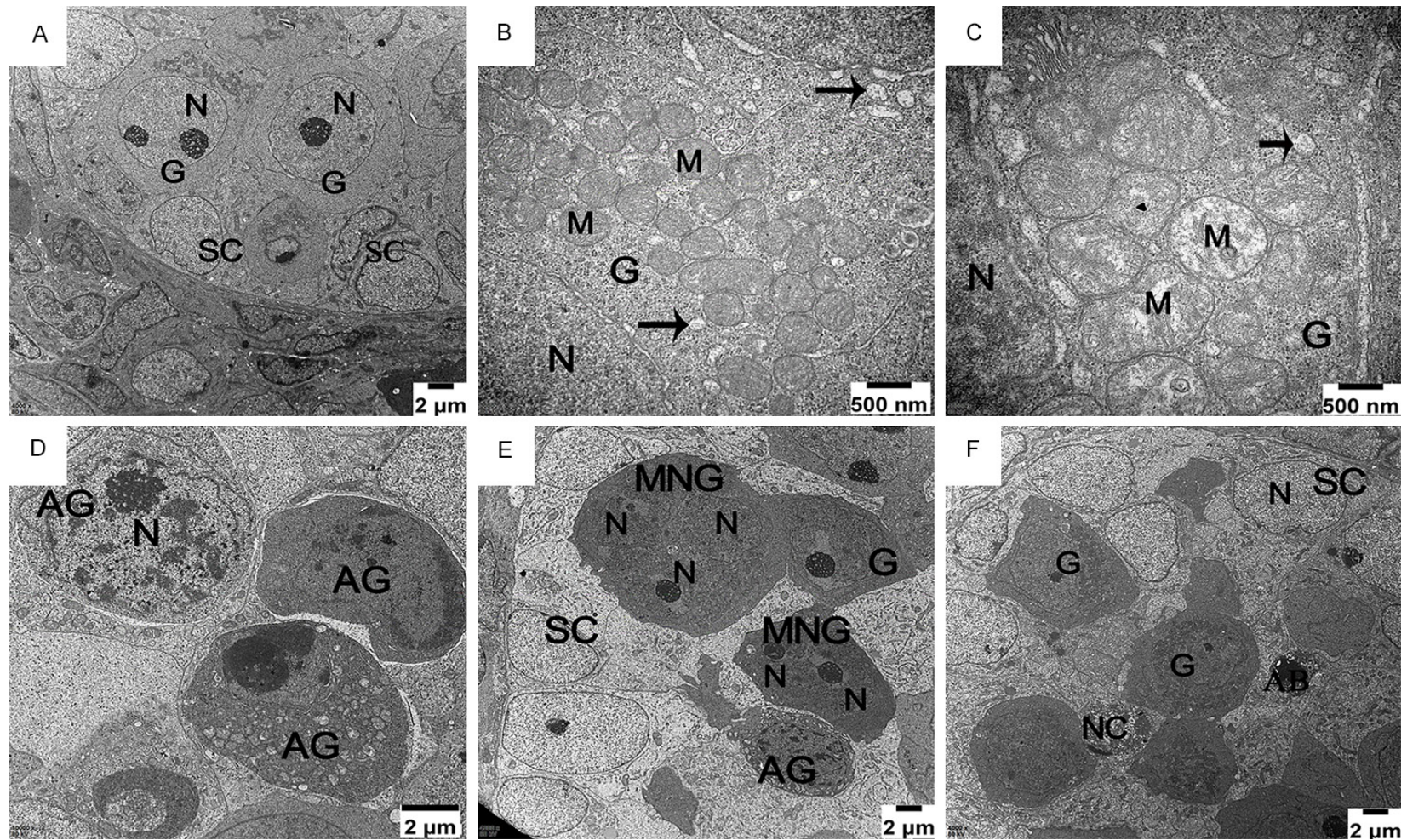


Figure 3. Ultrastructural changes of gonocytes (G) after MEHP treatment. A, B. Normal ultrastructure of gonocytes was shown in the control group. C. Swollen mitochondria (M) with loss of cristae were observed after MEHP treatment. D, E. Apoptotic gonocytes (AG) and multinucleated gonocytes (MNG) were observed after MEHP treatment. F. The electron density of many gonocytes increased. N: nuclei, SC: Sertoli cell, NC: necrotic cell, AB: apoptotic body.

Ultrastructural changes in rat testes after MEHP exposure

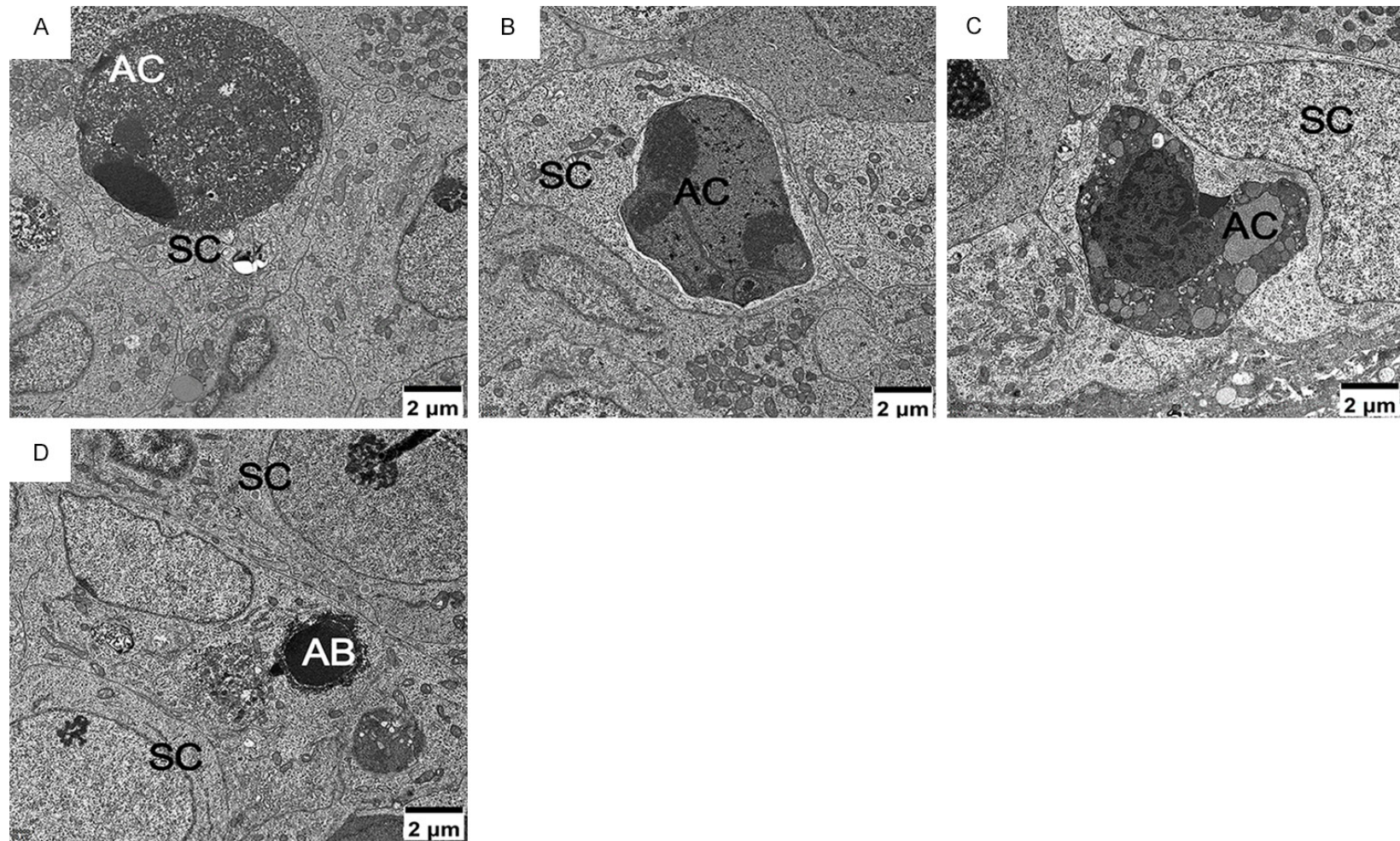


Figure 4. Ultrastructure of apoptotic cells (AC) and apoptotic body (AB) after MEHP treatment. A, B. Apoptotic cells were swallowed by adjacent Sertoli cells (SC). C. A Sertoli cell was swallowing an apoptotic cell. D. The apoptotic body was observed.

Ultrastructural changes in rat testes after MEHP exposure

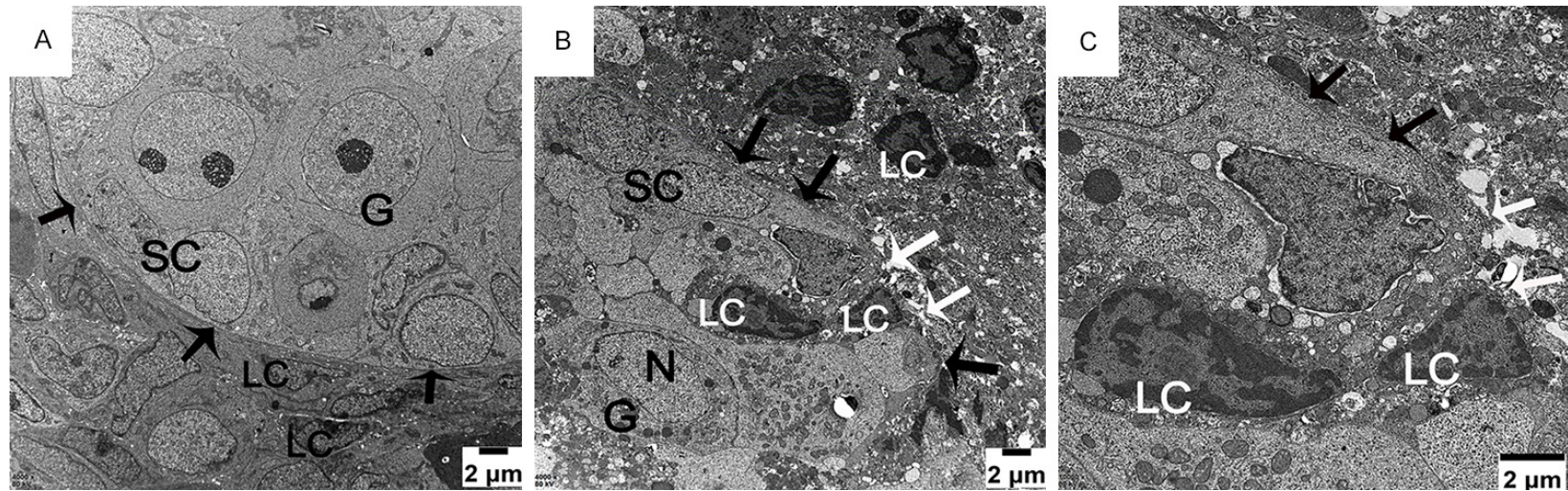


Figure 5. Degenerative changes of Leydig cells (LC) and basement membrane after MEHP treatment. A. Normal basement membrane (black arrow) was observed in the control group. B, C. After MEHP treatment, the basement membrane was broken (white arrow) and some nearby Leydig cells (LC) got in the seminiferous tubule. G: gonocyte, SC: Sertoli cells.

whereas most gonocytes were located at the center of seminiferous tubules and were larger in size than Sertoli cells [10, 18]. MEHP exposure initially damages the Sertoli cells; subsequently, the gonocytes are damaged due to impaired Sertoli cells [13, 21, 22]. In this study, after MEHP exposure, the first degenerative change was mitochondrial swelling in Sertoli cells. With exposure level increasing, MNGs and degenerative cells were observed. The occurrence of MNGs is an evident change of the “phthalate syndrome” in rodents and is considered to be independent of phthalate-induced decreased testosterone [23, 24].

The potential mechanism of occurrence of MNGs may be related to the interference of the membrane interactions between gonocytes and Sertoli cells. Mitochondrial swelling would disturb the function of Sertoli cells and lead to the appearance of MNGs. The migration of gonocytes guided by Sertoli cells from the center to the periphery of the seminiferous tubules is crucial for their normal differentiation and survival. Gonocytes remaining at the center of the tubule after 5 days postpartum are targeted for apoptosis [25-27]. MNGs which have difficulty in migrating towards the basement membrane due to their large volume and damaged Sertoli cells would be destined for apoptosis [13, 28]. Moreover, dysfunctional Sertoli cells do not effectively support the gonocytes and transmit an apoptotic signal to induce the death of gonocytes [18].

We observed an increased electron density of gonocytes named dark cells with no blebbing of the plasma, mitochondrial swelling, or distention of endoplasmic reticula. Dark-cell degeneration has been described in the degeneration of neuronal cells and chondrocytes; it was reported to be an apoptosis-like and hypoxia-related type of cell degeneration [29, 30]. Neurons undergoing dark-cell degeneration scarcely expressed caspase-3 [31]. Therefore, these dark cells are not identical to the classical apoptotic cells. However, it remains unclear whether dark cells could result in the loss of gonocytes and whether they represent the early stage of apoptotic cells.

After MEHP treatment at 100 μ M, we also observed ITLCs, which is consistent with previous studies [12, 32]. One study indicated that

fetal Leydig cells were just trapped when seminiferous tubules formed [32]. In this study, the basement membrane of the seminiferous tubule was broken, which facilitated the entry of Leydig cells into the seminiferous tubules. It is likely that fetal Leydig cells invaded the seminiferous tubules due to the impaired structural integrity of the basement membrane.

The functional significance of the ITLCs is still unclear. ITLCs may interfere with the normal development of Sertoli cells and disturb gonocytes' long-term survival and normal spermatogenesis, resulting in the appearance of Sertoli-cell-only tubules in adulthood [32, 33]. Moreover, ITLCs have also been observed in cryptorchids and patients with Sertoli-cell-only syndrome (SCOS) [34, 35]. Therefore, ITLCs may be a credible signal of testicular hypoplasia. On the other hand, testosterone production is disrupted after exposure to MEHP or in patients with cryptorchidism and SOCS. Testosterone can easily reach the tubular lumen if Leydig cells are located within the tubules. Therefore, the occurrence of ITLCs may represent a mechanism to compensate for impaired testosterone production [34].

To summarize, our research indicated that MEHP exposure induces deleterious ultrastructural effects in rat fetal testes; such as apoptosis, MNGs, and ITLCs, which provides additional insight into the ultrastructural changes related to the testicular toxicity of MEHP. Further studies are required to fully understand the mechanisms involved in MEHP-induced reproductive toxicity.

Acknowledgements

This work was supported by National Natural Science Foundation of China (Grant no. 81471446). We thank Mingxia Chen for her technical assistance.

Disclosure of conflict of interest

None.

Address correspondence to: Dr. Zi-Ming Wang, Department of Urology, The Second Affiliated Hospital, Xi'an Jiaotong University, Xi'an 710004, Shaanxi, China. Tel: +86-029-87679589; Fax: +86-029-87679533; E-mail: ziming-w@263.net

Ultrastructural changes in rat testes after MEHP exposure

References

- [1] DiVall SA. The influence of endocrine disruptors on growth and development of children. *Curr Opin Endocrinol Diabetes Obes* 2013; 20: 50-55.
- [2] Hauser R, Skakkebaek NE, Hass U, Toppari J, Juul A, Andersson AM, Kortenkamp A, Heindel JJ and Trasande L. Male reproductive disorders, diseases, and costs of exposure to endocrine-disrupting chemicals in the European Union. *J Clin Endocrinol Metab* 2015; 100: 1267-1277.
- [3] Toppari J, Larsen JC, Christiansen P, Giwercman A, Grandjean P, Guillette LJ Jr, Jegou B, Jensen TK, Jouannet P, Keiding N, Leffers H, McLachlan JA, Meyer O, Muller J, Rajpert-De Meyts E, Scheike T, Sharpe R, Sumpter J and Skakkebaek NE. Male reproductive health and environmental xenoestrogens. *Environ Health Perspect* 1996; 104 Suppl 4: 741-803.
- [4] Lambrot R, Muczynski V, Lecureuil C, Angenard G, Coffigny H, Pairault C, Moison D, Frydman R, Habert R and Rouiller-Fabre V. Phthalates impair germ cell development in the human fetal testis in vitro without change in testosterone production. *Environ Health Perspect* 2009; 117: 32-37.
- [5] Hermo L, Pelletier RM, Cyr DG and Smith CE. Surfing the wave, cycle, life history, and genes/proteins expressed by testicular germ cells. Part 1: background to spermatogenesis, spermatogonia, and spermatocytes. *Microsc Res Tech* 2010; 73: 241-278.
- [6] Cheng CY and Mruk DD. Cell junction dynamics in the testis: sertoli-germ cell interactions and male contraceptive development. *Physiol Rev* 2002; 82: 825-874.
- [7] Culty M. Gonocytes, the forgotten cells of the germ cell lineage. *Birth Defects Res C Embryo Today* 2009; 87: 1-26.
- [8] Culty M. Gonocytes, from the fifties to the present: is there a reason to change the name? *Biol Reprod* 2013; 89: 46.
- [9] Stroheker T, Regnier JF, Lassarguere J and Chagnon MC. Effect of in utero exposure to di-(2-ethylhexyl)phthalate: distribution in the rat fetus and testosterone production by rat fetal testis in culture. *Food Chem Toxicol* 2006; 44: 2064-2069.
- [10] Livera G, Delbes G, Pairault C, Rouiller-Fabre V and Habert R. Organotypic culture, a powerful model for studying rat and mouse fetal testis development. *Cell Tissue Res* 2006; 324: 507-521.
- [11] Habert R, Muczynski V, Grisin T, Moison D, Messiaen S, Frydman R, Benachi A, Delbes G, Lambrot R, Lehraiki A, N'Tumba-Byn T, Guerquin MJ, Levacher C, Rouiller-Fabre V and Livera G. Concerns about the widespread use of rodent models for human risk assessments of endocrine disruptors. *Reproduction* 2014; 147: R119-129.
- [12] Chauvigne F, Menuet A, Lesne L, Chagnon MC, Chevrier C, Regnier JF, Angerer J and Jegou B. Time- and dose-related effects of di-(2-ethylhexyl) phthalate and its main metabolites on the function of the rat fetal testis in vitro. *Environ Health Perspect* 2009; 117: 515-521.
- [13] Muczynski V, Cravedi JP, Lehraiki A, Levacher C, Moison D, Lecureuil C, Messiaen S, Perdu E, Frydman R, Habert R and Rouiller-Fabre V. Effect of mono-(2-ethylhexyl) phthalate on human and mouse fetal testis: in vitro and in vivo approaches. *Toxicol Appl Pharmacol* 2012; 261: 97-104.
- [14] Lambrot R, Coffigny H, Pairault C, Donnadiou AC, Frydman R, Habert R and Rouiller-Fabre V. Use of organ culture to study the human fetal testis development: effect of retinoic acid. *J Clin Endocrinol Metab* 2006; 91: 2696-703.
- [15] Chauvigne F, Plummer S, Lesne L, Cravedi JP, Dejucq-Rainsford N, Fostier A and Jegou B. Mono-(2-ethylhexyl) phthalate directly alters the expression of Leydig cell genes and CYP17 lyase activity in cultured rat fetal testis. *PLoS One* 2011; 6: e27172.
- [16] Latini G, De Felice C, Presta G, Del Vecchio A, Paris I, Ruggieri F and Mazzeo P. In utero exposure to di-(2-ethylhexyl)phthalate and duration of human pregnancy. *Environ Health Perspect* 2003; 111: 1783-1785.
- [17] Lin L, Zheng LX, Gu YP, Wang JY, Zhang YH and Song WM. Levels of environmental endocrine disruptors in umbilical cord blood and maternal blood of low-birth-weight infants. *Zhonghua Yu Fang Yi Xue Za Zhi* 2008; 42: 177-180.
- [18] Li H and Kim KH. Effects of mono-(2-ethylhexyl) phthalate on fetal and neonatal rat testis organ cultures. *Biol Reprod* 2003; 69: 1964-1972.
- [19] Elmore S. Apoptosis: a review of programmed cell death. *Toxicol Pathol* 2007; 35: 495-516.
- [20] Schenk RL, Strasser A and Dewson G. BCL-2: long and winding path from discovery to therapeutic target. *Biochem Biophys Res Commun* 2017; 482: 459-469.
- [21] Erkekoglu P, Zeybek ND, Giray B, Asan E and Hincal F. The effects of di(2-ethylhexyl)phthalate exposure and selenium nutrition on sertoli cell vimentin structure and germ-cell apoptosis in rat testis. *Arch Environ Contam Toxicol* 2012; 62: 539-547.
- [22] Andriana BB, Tay TW, Maki I, Awal MA, Kanai Y, Kurohmaru M and Hayashi Y. An ultrastructural study on cytotoxic effects of mono(2-ethylhexyl) phthalate (MEHP) on testes in Shiba goat in vitro. *J Vet Sci* 2004; 5: 235-240.

Ultrastructural changes in rat testes after MEHP exposure

- [23] Gaido KW, Hensley JB, Liu D, Wallace DG, Borghoff S, Johnson KJ, Hall SJ and Boekelheide K. Fetal mouse phthalate exposure shows that Gonocyte multinucleation is not associated with decreased testicular testosterone. *Toxicol Sci* 2007; 97: 491-503.
- [24] Mahood IK, Scott HM, Brown R, Hallmark N, Walker M and Sharpe RM. In utero exposure to di(n-butyl) phthalate and testicular dysgenesis: comparison of fetal and adult end points and their dose sensitivity. *Environ Health Perspect* 2007; 115 Suppl 1: 55-61.
- [25] Tres LL and Kierszenbaum AL. The ADAM-integrin-tetraspanin complex in fetal and post-natal testicular cords. *Birth Defects Res C Embryo Today* 2005; 75: 130-141.
- [26] van den Driesche S, McKinnell C, Calarao A, Kennedy L, Hutchison GR, Hrabalkova L, Jobling MS, Macpherson S, Anderson RA, Sharpe RM and Mitchell RT. Comparative effects of di(n-butyl) phthalate exposure on fetal germ cell development in the rat and in human fetal testis xenografts. *Environ Health Perspect* 2015; 123: 223-230.
- [27] Kleymenova E, Swanson C, Boekelheide K and Gaido KW. Exposure in utero to di(n-butyl) phthalate alters the vimentin cytoskeleton of fetal rat Sertoli cells and disrupts Sertoli cell-gonocyte contact. *Biol Reprod* 2005; 73: 482-490.
- [28] Orth JM, Jester WF, Li LH and Laslett AL. Gonocyte-Sertoli cell interactions during development of the neonatal rodent testis. *Curr Top Dev Biol* 2000; 50: 103-124.
- [29] Leist M and Jaattela M. Four deaths and a funeral: from caspases to alternative mechanisms. *Nat Rev Mol Cell Biol* 2001; 2: 589-598.
- [30] Roach HI and Clarke NM. Physiological cell death of chondrocytes in vivo is not confined to apoptosis. New observations on the mammalian growth plate. *J Bone Joint Surg Br* 2000; 82: 601-613.
- [31] Yang DS, Kumar A, Stavrides P, Peterson J, Peterhoff CM, Pawlik M, Levy E, Cataldo AM and Nixon RA. Neuronal apoptosis and autophagy cross talk in aging PS/APP mice, a model of Alzheimer's disease. *Am J Pathol* 2008; 173: 665-681.
- [32] Mahood IK, McKinnell C, Walker M, Hallmark N, Scott H, Fisher JS, Rivas A, Hartung S, Ivell R, Mason JI and Sharpe RM. Cellular origins of testicular dysgenesis in rats exposed in utero to di(n-butyl) phthalate. *Int J Androl* 2006; 29: 148-154; discussion 181-145.
- [33] Mahood IK, Hallmark N, McKinnell C, Walker M, Fisher JS and Sharpe RM. Abnormal Leydig Cell aggregation in the fetal testis of rats exposed to di (n-butyl) phthalate and its possible role in testicular dysgenesis. *Endocrinology* 2005; 146: 613-623.
- [34] Mori H, Tamai M, Fushimi H, Fukuda H and Maeda T. Leydig cells within the aspermatogenic seminiferous tubules. *Hum Pathol* 1987; 18: 1227-1231.
- [35] Schulze C and Holstein AF. Leydig cells within the lamina propria of seminiferous tubules in four patients with azoospermia. *Andrologia* 1978; 10: 444-452.